SAE INTERNATIONAL

ARTICLE INFO
Article ID: 13-02-01-0002

doi:10.4271/13-02-01-0002

Eco-Approach and Departure along Signalized Corridors Considering Powertrain Characteristics

Guoyuan Wu,[1] Peng Hao,[1] Ziran Wang,[1] Yu Jiang,[1] Kanok Boriboonsomsin,[1] Matthew Barth,[1] Michael McConnell,[2] Shuwei Qiang,[3] and John Stark[2]

[1]University of California Riverside, USA
[2]Leidos, Inc., USA
[3]Amazon, Inc., USA

Abstract

With the emergence of connected and automated vehicles (CAVs), numerous dynamic eco-driving strategies have been developed all over the world. The Eco-Approach and Departure (EAD) application is considered to be a promising solution to the relief of transportation activity-related pressure on energy and environment. Unlike most of existing EAD strategies that utilize signal phase and timing (SPaT) information on an intersection basis, we propose a computationally efficient algorithm for EAD along signalized corridors (EADSC), which can take advantage of SPaT information of all the intersections along the corridor as a whole, and can determine the optimal (in terms of fuel efficiency) speed trajectories with the consideration of the host vehicle's powertrain characteristics. Both the numerical study and real-world field implementation indicate that the proposed EADSC system shows great promise in fuel savings (e.g., ranging from 12% to 28%) without compromising on mobility, compared to the baseline driving strategy without SPaT knowledge and other representative EAD strategies. We also discuss some practical issues when deploying the proposed system in the real-world, such as unavailability of complete knowledge on the background signal timing plan in current SPaT messages, and handling of interactions from other traffic (e.g., cut-ins).

History

Received: 09 Aug 2020
Revised: 05 Nov 2020
Accepted: 11 Jan 2021
e-Available: 18 Mar 2021

Keywords

Connected and automated vehicle (CAV), Dynamic eco-driving, Signal phase and timing (SPaT), Signalized corridor

Citation

Wu, G., Hao, P., Wang, Z., Jiang, Y. et al., "Eco-Approach and Departure along Signalized Corridors Considering Powertrain Characteristics," *SAE Int. J. Sust. Trans., Energy, Env., & Policy* 2(1):2021, doi:10.4271/13-02-01-0002.

ISSN: 2640-642X
e-ISSN: 2640-6438

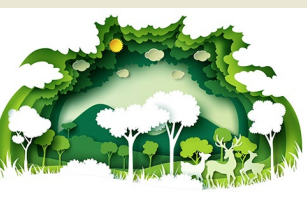



1. Introduction

The uninterrupted growth in transportation activities, for both people and goods movement, has been exerting a significant amount of pressure on our society, economy, and environment. It was reported that about 28% of total U.S. energy was consumed for transporting people and goods from one place to another in 2018 [1]. In addition, according to a report by U.S. Environmental Protection Agency (USEPA), the transportation sector accounted for 28% of total greenhouse gas (GHG) emissions in 2018, higher than any other sector including electricity, industry, agriculture, commercial, and residential [2].

On the other hand, emerging technologies such as connected vehicles (CVs), transportation electrification, and edge computing have been stimulating more and more dedicated efforts by engineers, researchers, and policymakers to tackle these transportation-related energy and environmental problems. Good examples include the Applications for the Environment: Real-Time Information Synthesis (AERIS) Program initiated by U.S. Department of Transportation [3], the eCoMove [4], and Horizon 2020 [5] funded by the European Commission. A variety of environmentally friendly CV applications [6], in particular those related to eco-driving strategies, have been proposed, developed, and validated. Among all eco-driving strategies, the Eco-Approach and Departure at Signalized Intersections (EADSI) system has shown significant promise [7, 8, 9, 10, 11]. In this system, an equipped vehicle can take advantage of the signal phase and timing (SPaT) and geometric intersection description (GID) information from the upcoming signalized intersection, and then calculate the optimal speed profile to pass through the intersection in green or to decelerate to a full stop in the most energy efficient manner. Speed references may be provided to the driver using a driver-vehicle interface (DVI) or to the control system that supports automated driving capabilities (at least) longitudinally.

Due to its attractiveness, the eco-driving system has received considerable attention from numerous studies involved in the development and testing of various algorithms [12, 13, 14, 15, 16, 17, 18, 19, 20, 21]. However, many of these algorithms are not flexible enough to handle well the road grade, customized powertrain characteristics, or interaction with other traffic. In addition, very few of them have been designed and validated for eco-driving along signalized corridors but only for isolated intersections [22]. Their extendibility to handle the eco-driving along multiple signalized intersections is still questionable, mainly due to the real-time performance.

To address the aforementioned issues, we propose herein an innovative algorithm for Eco-Approach and Departure along Signalized Corridors (EADSC). Unlike EADSI, the proposed EADSC can take full advantage of the SPaT information from all downstream intersections (e.g., via cellular communications) to plan the equipped vehicle's trajectory. More specifically, it is assumed that the downstream traffic states can be reliably predicted (through the fusion of all available sensors). This predicted information can be integrated with the host vehicle's states and characteristics (e.g., location, instantaneous speed, tractive power limit) to construct the so-called reachable region (RR) at the lane level. Based on the predicted lane-level RR, the optimal passage cycle (in terms of energy/fuel consumption minimization with consideration of detailed powertrain characteristics) at each signal can be determined in a time-efficient manner, to guarantee the real-time performance of the EADSC algorithm. Upon the determination of the target cycle at each signal along the corridor, the RR can be significantly reduced.

Then, the trajectory planning can be formulated as a shortest path problem within the reduced RR.

The rest of this article is organized as follows: Section 2 reviews the background information related to the proposed EADSC system. Details of the methodology are described in Section 3, followed by the (numerical) case study in Section 4. The field implementation is presented in Section 5. Section 6 discusses some practical issues for real-world deployment. The last section summarizes this article with concluding remarks and future work.

2. Literature Review and Background

In this section, we first review the status quo of research related to EAD application, and then give a brief introduction on the powertrain model used for fuel/energy consumption estimation in this study.

2.1. Eco-Approach and Departure

In the past decade, a variety of studies have been conducted on EAD, especially from the perspective of isolated intersections. Mandava et al. [12] proposed a piecewise linear trigonometric function-based vehicle trajectory planning algorithm for eco-driving along urban arterials. It has been extensively evaluated and validated in both simulation [23] and field testing (with light-duty vehicle [24] and heavy-duty truck [25], respectively), in the form of either advanced driver assistance system (ADAS) [26] or partially automated control [27], showing good real-time performance and substantial benefits in reducing fuel consumption and tailpipe emissions. However, significant efforts are required to modify the algorithm to accommodate customized powertrain models and to handle rolling terrains. Based on the VT-Micro model, Rakha and Kamalanathsharma [14] developed a constant deceleration-based eco-driving strategy to avoid full stops at signals, followed by further improvement using a multistage dynamic programming and recursive path-finding principles as well as evaluation with an agent-based model [28]. Asadi and Vahidi [15] proposed a two-step predictive cruise control concept, aiming to reduce fuel use and trip time by utilizing

traffic signal status information. The first step is to determine the target speed based on available green window, while the second step is to perform the optimal tracking of target speed. Katsaros et al. [16] developed a Green Light Optimized Speed Advisory (GLOSA) system whose goal was to minimize average fuel consumption and average stop delay at a traffic signal. By taking into account the queue discharging process, Chen et al. [17] devised an eco-driving algorithm for the equipped vehicle's approaching and leaving a signalized intersection to minimize the integrated metrics of emissions and travel time, but the algorithm did not consider the roadway grade information. Jin et al. [18] formulated the power-based optimal eco-driving problem as a 0-1 Binary Mixed Integer Linear Programming (MILP), which is applicable to scenarios of signalized intersection, nonsignalized intersection, or freeway. The approach can take into account road-grade effects and powertrain dynamics, but has relatively low computational efficiency. Li et al. [19] used the Legendre pseudospectral method and knotting technique to overcome the discrete gear ratio issue in the optimal control for eco-driving at signalized intersections. Huang and Peng [20] adopted a simplified powertrain model and applied the sequential convex optimization approach to optimizing vehicle speed trajectory at signalized intersections, which can keep a balance between optimality and real-time performance.

When considering the application of EAD in a more realistic environment, many studies took "reactive" approaches to cope with disturbances from the downstream traffic (e.g., switching to the car-following mode control if the host vehicle was too close to its predecessor) or assumed traffic signals were running fixed-time mode [21, 29, 30]. To address these issues, some researchers specifically focused on tackling the queuing effects for EADSI by applying the shockwave theory [31] or data-driven techniques [32] to predict the queue length or in essence the trajectory of the host vehicle's predecessor. Others were dedicated to dealing with uncertainties in traffic signal operation such as actuated signals by improving the prediction of the SPaT information [33] or developing more robust eco-driving strategies [34, 35, 36]. In addition, most of the existing EAD strategies were applicable to only isolated intersection scenarios or to signalized corridor scenarios, but in an intersection-by-intersection manner which may be far from being optimal. Very few studies were particularly focused on the eco-driving strategies along multiple signalized intersections [35, 37, 38, 39], where one of the major challenges was to balance energy minimization against computational efficiency for driving on a long enough roadway stretch. Some recent studies tried to address the real-time performance for dynamic eco-driving along the signalized corridor [22, 40], but the selected speed profiles were simplified with certain smoothness assumptions without considering detailed powertrain characteristics. In this article, we develop a flexible algorithm for EADSC, which can accommodate a variety of factors (e.g., customized powertrain, rolling terrain, disturbance from downstream traffic, and uncertainty in signal operation), while keeping the balance between optimality and real-time performance.

2.2. Powertrain Model and Fuel Consumption Estimation

One of the key questions in vehicle trajectory planning for EAD is to identify a useful model, which directly relates the energy consumption rate with the vehicle dynamics and other externalities such as road grade, wind speed, and road surface roughness. On one hand, the longitudinal vehicle dynamics model [41] governs the relationship between the traction/brake force (F_t) and the inertia force (F_i) as well as other road resistances, including rolling resistance (F_f), aerodynamic drag (F_a), and grade resistance (F_g):

$$F_t(v,a,\theta) = F_i + F_f + F_a + F_g = \delta ma + mgf_r \cos\theta + \frac{1}{2}\rho_a C_D A_f v^2 + mg\sin\theta \quad \text{Eq. (1)}$$

where m represents the vehicle mass; S is the coefficient accounting for the effect of rotating and reciprocating parts; g is the gravity factor (m/s^2); f_r is the rolling resistance coefficient; θ is the road grade (rad); C_D is the drag coefficient; ρ_a is the air density (kg/m^3); A_f is the vehicle frontal area (m^2); and v is the vehicle speed (m/s).

On the other hand, the engine efficiency map or brake-specific fuel consumption (see Figure 1 as an example) sets up the mapping from both engine torque (τ) and engine speed (ω) to the fuel consumption rate (Q). In this study, we use activity dataset collected from the test vehicle to fit the energy consumption rate (liter/h) as a quadratic function of engine torque (N·m) and engine speed (rpm):

$$Q_t(\tau,\omega) = \beta_1 + \beta_2\tau + \beta_3\omega + \beta_4\tau\omega + \beta_5\tau^2 + \beta_6\omega^2 \quad \text{Eq. (2)}$$

where β_i represents the coefficient of the ith terms in Equation 2.

Therefore, to map the fuel consumption rate with vehicle speed, acceleration and road grade, that is, $Q_t(v, a, \theta)$,

FIGURE 1 An example engine map where the maximum engine torque-speed curve is indicated by the solid curve.

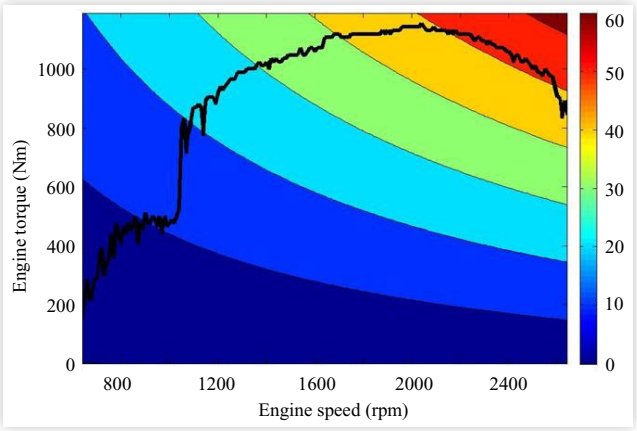

we approximate both engine torque and engine speed as functions of these variables. One key step is to relate the "lumped" gear ratio as a function of vehicle speed, as both engine torque and engine speed can be expressed as

$$\tau = \frac{F_t(v,a,\theta)}{\eta n} = \frac{1}{\eta n}\left(\delta ma + mgf_r\cos\theta + \frac{1}{2}\rho_a C_D A_f v^2 + mg\sin\theta\right) \quad \text{Eq. (3)}$$

$$\omega = n \cdot v \quad \text{Eq. (4)}$$

where η is the overall powertrain efficiency; and the "lumped" gear ratio $n = r_f r_t / r_r$ is determined by the final drive ratio r_f, the gear ratio of the transmission r_t, and the radius of wheel r_r. By following the similar step in [42], we formulate the "lumped" gear ratio as the sum of weighted indicator functions of v where the weights are the ratios at associated gear levels. It is also noted that if the vehicle is operating in the coast or brake mode, that is, $\frac{dv}{dt} \le a_{coast}$, then we assume the fuel consumption rate is a constant Q_{idie} which equals to the rate when idling, and

$$a_{coast} = -mgf_r\cos\theta - \frac{1}{2}\rho_a C_D A_f v^2 - -mg\sin\ \theta \quad \text{Eq. (5)}$$

3. Proposed Methodology

Figure 2 presents a flowchart of the framework that enables an equipped vehicle to perform dynamic eco-driving along a signalized corridor, which includes the stages of sensing, planning (or decision-making), and execution. In this study, we focus on the development and validation of three major steps of our EADSC algorithm (i.e., planning stage): (a) *RR construction*; (b) *target cycle determination*; and (c) *vehicle trajectory planning*. The *environment sensing*, lane-level *traffic state prediction* (including sensor fusion), and *execution and state update* (e.g., low-level controller design) are also important topics, but outside the scope of this study. Before elaborating the description of each step, a few major assumptions and remarks are presented in the following:

- The traffic signal controllers along the corridor are operating in fixed-time manner. Therefore, the SPaT information is deterministic and the future signal state can be well predicted. It is expected that actuated signal control would present much more challenges for eco-driving due to some uncertainties in the future SPaT, as discussed in our previous research [34].
- Full knowledge of background signal timing (i.e., cycle length, phase duration, phase sequence) is available for trajectory planning. This is a widely adopted assumption for almost all EAD-related studies. However, this information may not be available in the SPaT message in practice [43]. Further discussion on how to handle partial knowledge of background signal timing from the SPaT will be presented in Section 6.

3.1. Reachable Region Construction

In this study, we define the lane-level "Reachable Region" (with respect to the host vehicle) as the set of (predicted) reachable states in the spatiotemporal region or distance-time (D-T) diagram, which is widely used in the transportation engineering (see the "void" areas in Figure 3). The figure may represent one ingress lane along the approach of interest at a signalized intersection with potential disturbances from other traffic. As can be observed in the figure, the RR is usually bounded due to both endogenous and exogenous factors. The endogenous factors may include the host vehicles' tractive power limit, maximum acceleration/deceleration, and jerk limit to guarantee driving comfort, while the exogenous factors consider the roadway speed limit, (predicted) downstream traffic conditions (such as queue length or predecessor's trajectory), and the upcoming traffic SPaT.

FIGURE 2 Flowchart of the proposed methodology.

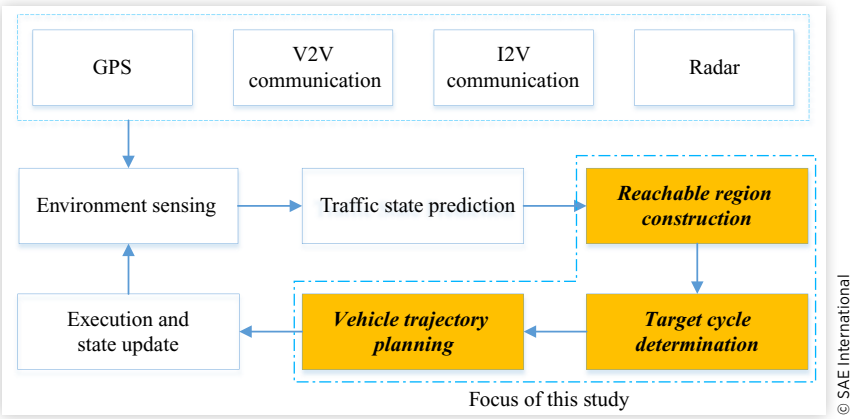

FIGURE 3 An example of the reachable region for approaching a signalized intersection.

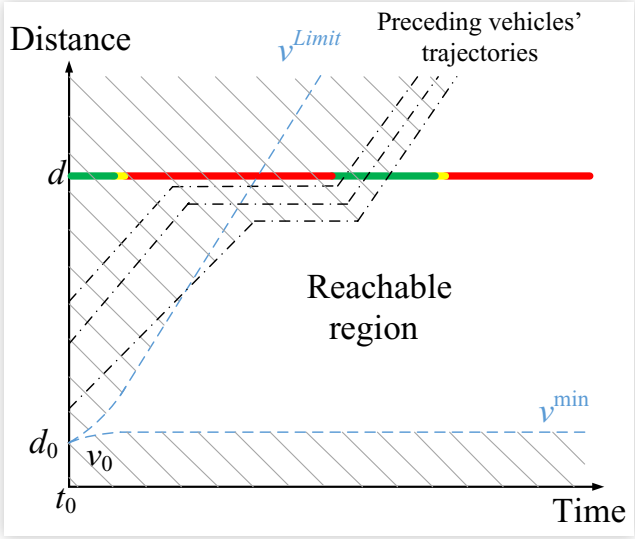

For eco-driving along a signalized corridor, the major purpose of the *RR construction* algorithm is to reduce the size of feasible region for the host vehicle's trajectory planning, in particular the size of searching space for available green phases (within different cycles) at each signalized intersection along the corridor, by applying any aforementioned system constraints (e.g., speed limit, no collision to preceding vehicles). The key output of the *RR construction* algorithm is a set of intervals $\left[t_i^{\min}, t_i^{\max}\right]$, where $t_i^{\min}$ represents the earliest feasible crossing time at the stop line of the ith downstream intersection, while $t_i^{\max}$ is the latest feasible crossing time at the same intersection considering a nontrivial minimum cruising speed $v^{\min}$ (e.g., to avoid presenting potential safety hazards to other traffic). When the host vehicle is traveling in traffic, the crossing time of its exact proceeding vehicle t_i' needs to be predicted and the minimum headway $h^{\min}$ should be considered to estimate $t_i^{\min}$. Inspired by [39], the lane-level *RR construction* algorithm is proposed to include: (1) forward calculation of $t_i^{\min}$ based on $t_{i-1}^{\min}$ and t_i' and (2) backward correction of $t_i^{\max}$ to avoid any constraint violation. If there is no feasible solution (i.e., the set is empty at certain signal), then a nonstop trajectory along the signalized corridor is very unlikely. Also note that the algorithm is based on the assumption that the host vehicle has full knowledge of all the signal timing plans (under fixed-time control) along the corridor, and the preceding vehicle's trajectory is well predicted.

Since the *RR construction* algorithm is performed at the lane level where the queue length is already taken into account, we could further develop "proactive" lane selection and lane change strategies (e.g., queue balancing or overtaking) for the real-world situation to help the host vehicle identify or update its passage path (in the D-T diagram) along the corridor, rather than changing the lane in a "reactive" manner (e.g., to avoid collision or a wrecked vehicle/object). The lateral maneuver is not the focus of this study, but can definitely be one of the future steps.

3.2. Target Cycle Determination

Once we construct the RR in the D-T diagram, we discretize it in both space and time to find the optimal vehicle trajectory. For an isolated intersection, the size of RR should be acceptable considering the computational efficiency. However, as route length and the number of intersections along the target corridor increase, the RR will expand dramatically, and the real-time performance for vehicle trajectory planning becomes questionable. Therefore, we develop the *target cycle determination* step to quickly identify the target cycle that the optimal vehicle trajectory should pass at each intersection. Since we assume all the signal plans of downstream intersections are available, this problem can be formulated to find the optimal path from the initial states (i.e., d_0 and v_0) at time t_0 to some final states (where d_f and v_f are supposed to be given, and the knowledge of t_f is optional) within the RR in a weighted directed acyclic graph (see Figure 4).

Figure 4 illustrates an example of the case considering roadway speed limit v^{Limit} and nontrivial minimum cruising speed $v^{\min}$, but no other traffic interaction. The node ("blue dot") represents feasible passage time within the green phase of each cycle at the respective signalized intersection. In this figure, the node is placed at the beginning of each feasible green window. For a better approximation, more nodes (e.g., the mid-point and end point) can be placed within the same green phase. The number of candidate nodes would heavily depend on the fineness of approximation as well as real-time performance requirement on this step.

As aforementioned, the purpose of this step is to determine which cycle the host vehicle should travel through to achieve the minimal energy consumption in a time-efficient manner, rather than finding the exact optimal passage time at each intersection. We use parabolic speed profiles (as shown in Equations 6 and 7) to smoothly (in terms of speed and acceleration) connect each signalized intersection (in the D-T diagram) along the corridor, where the vehicle speed at (t_0, d_0) is v_0 and the vehicle speed at (t_i, d_i) for $i = 1, 2, 3, \ldots$ is v_i^f, which can be the roadway speed limit v^{Limit}, a user-defined free-flow speed, or an intermediate value between $v^{\min}$ and v^{Limit} (varied with intersection). More specifically, the proposed parabolic speed trajectories are as follows ($t_0 = 0$ without loss of generality):

Between d_0 and d_1:

$$v(t) = a_1 t^2 + b_1 t + c_1, \quad t \in [0,\ t_1) \qquad \text{Eq. (6)}$$

where

$$a_1 = \frac{3}{t_1^2}\left(v_0 + v_i^f\right) - \frac{6\left(d_1 - d_0\right)}{t_1^3}$$

$$b_1 = \frac{1}{t_1}\left(v_1^f - v_0\right) - a_1 t_1$$

$$c_1 = v_0$$

FIGURE 4 Possible passage cycle combinations along the signalized corridor [44].

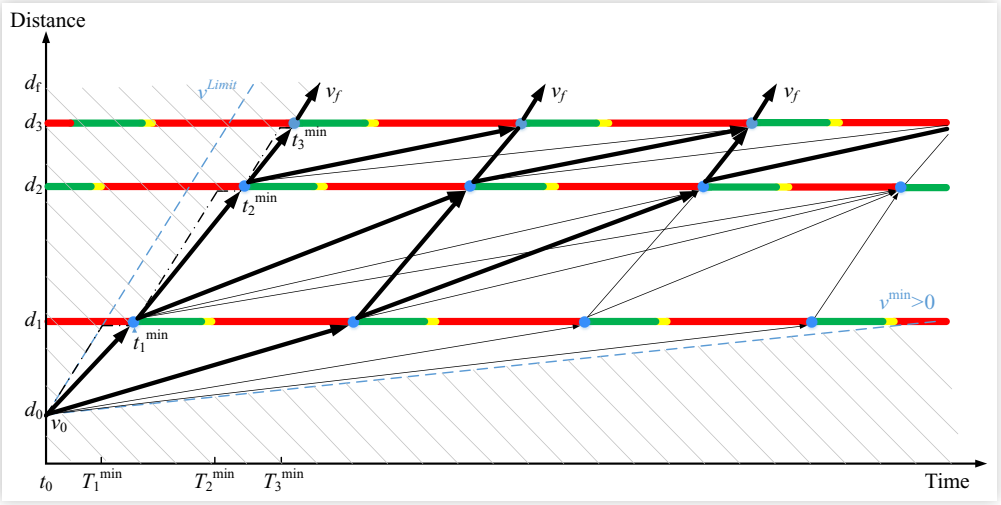

Reprinted with permission from Ref. [44].

Between d_i and d_{i+1} ($i = 1, 2, 3, \ldots$):

$$v(t) = a_2 t^2 + b_2 t + c_2, t \in [t_i, t_{i+1}) \qquad \text{Eq. (7)}$$

where

$$a_2 = \frac{6v_i^f}{(t_{i+1} - t_i)^2} - \frac{6(d_{i+1} - d_i)}{(t_{i+1} - t_i)^3}$$
$$b_2 = -a_2(t_{i+1} - t_i)$$
$$c_2 = v_{i+1}^f$$

With the approximated speed profiles, we estimate the fuel/energy cost of each arc using the energy estimation model described in Section 2.2. Then, the problem is formulated as finding the shortest path with single origin and multiple destinations, which can be solved efficiently with the Dijkstra's algorithm [45]. If a target arrival time is also defined, then the problem can be reduced to a typical shortest path problem with single origin and single destination where more efficient algorithms (e.g., A* algorithm [46]) may be applied. As the determination of target passage cycle is an approximate process, it may not be necessary to have too many paths in real-world implementation. For example, we may only look at two cycles ahead from each accessible node at each intersection (see those thicker lines in Figure 4), without much compromising in mobility. In that case, even an enumerative searching may be computationally acceptable in real-world deployment. In the case where the full knowledge of signal plans of all downstream intersections is not available, the scope of graph model and the connectivity between nodes would be significantly constrained and need updating as new information flows in. This issue will be elaborated in Section 6.

3.3. Vehicle Trajectory Planning

After the determination of target passage cycle at each downstream intersection, the potential RR is significantly reduced. Within the reduced region (including the available green window at each intersection), we can formulate another weighted directed graph model $G = (V, E, C)$ where V, E, C represent the set of vertices, edges, and costs, respectively, by discretizing the time and space into fixed-time step Δt and distance grid Δx (therefore the speed is discretized with the step of $\Delta x/\Delta t$ for consistency). This is similar to the approach described in Section 3.2. For each node, we assign a 3-tuple (t, x, v), which describes the dynamic state of the host vehicle, where $t \in (0, T]$ is the time (in second); $x \in [0, L]$ is the traveled distance (in meter) along the entire route with the length of L; and $v \in [0, v^{Limit}]$ is the speed (in m/s). The edge defines the connectivity between two nodes, and $e_{V_i \to V_j}$ is created from $V_i(t_i, x_i, v_i)$ to $V_j(t_j, x_j, v_j)$ if and only if the following rules are satisfied:

- Consecutive in time, i.e., $t_j = t_i + \Delta t$
- Consistency between distance and speed: $x_j = x_i + v_i \Delta t$
- Boundary on acceleration and consistency between speed and acceleration, i.e.,

$$a_{\min} \le \frac{v_j - v_i}{\Delta t} \le a_{\max}$$

where $a_{\min}$ and $a_{\max}$ are the maximum deceleration rate and maximum acceleration rate for the host vehicle, respectively. The jerk constraint may be applied in a similar manner (if any).

Using the model presented in Section 2.2, we calculate the cost $c_{V_i \to V_j}$ on edge $e_{V_i \to V_j}$ as follows:

$$c_{V_i \to V_j} = \begin{cases} Q_t\left(v_{i'} \dfrac{v_j - v_i}{\Delta t}, \theta_i\right) & \text{if} \quad \dfrac{v_j - v_i}{\Delta t} > a_{coast} \\ Q_{idle} & \text{if} \quad \dfrac{v_j - v_i}{\Delta t} \le a_{coast} \end{cases} \qquad \text{Eq. (8)}$$

where the road grade θ_i can be estimated by the elevations between nodes V_i and V_j.

Upon the completion of this directed graph model, we then apply the Dijkstra's algorithm to solve this single source shortest path problem with nonnegative cost. Figure 5 illustrates an example where the host vehicle traverses a road segment (36 m long) in 4 s with both the initial and final speed being 10 m/s. The time step Δt is 1 s, the distance grid Δx is 2 m, and the maximum and minimum acceleration rates are 2 m/s^2 and −2 m/s^2, respectively. For a more generic case of EADSC where the RR has extended scope in space and time with higher resolution, the time complexity using the Dijkstra's algorithm is $O(\log(N)*E)$ [45], where N represents the number of nodes and E denotes the number of edges. The pseudocode for the *vehicle trajectory planning* algorithm is as follows.

FIGURE 5 An example to illustrate the *vehicle trajectory planning* step by constructing the graphic model and formulating it as the shortest path problem.

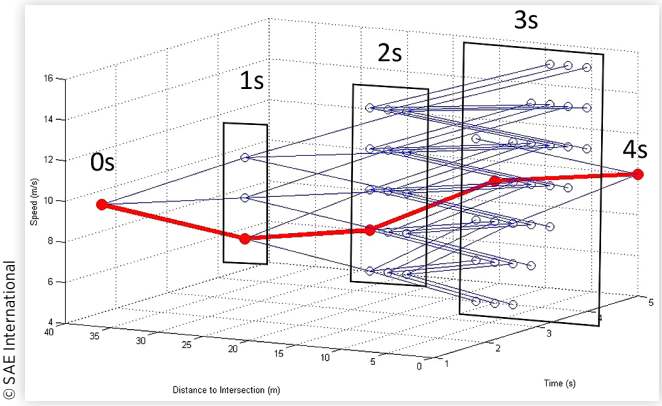

4. Numerical Simulation

To illustrate the performance of the proposed EADSC system, we conduct a numerical case study in this section using a three-intersection road stretch of El Camino Real in Palo Alto, CA, consisting of three cross-streets—Maybell Ave., Los Robles Ave., and Ventura Ave.—from south to north. The road-grade change is less than 1% (around 0.4%) and therefore

ALGORITHM *Vehicle Trajectory Planning* Algorithm

Input: vertices and edges (with associated weights) in the reachable region, host vehicle's initial and target states.
Output: least cost path connecting host vehicle's initial state with target one.
Initialize graph(vertex, edge, value) = null;
for each $(t, d) \in$ reachable region
  for each $v \in$ speed range
    graph.add_vertex $V(t, d, v)$;
  end
end
for $t = t_0$ to $t_d - 1$
  for each vertex $V(t, d_1, v_1)$
    for each vertex $V(t+1, d_2, v_2)$
      if $d_2 = d_1 + v_1$ & $v_2 - v_1 \ge v_{\min}$ & $v_2 - v_1 \ge a_{\max}$
        graph.add_edge($V(t, d_1, v_1)$ $V(t+1, d_2, v_2)$);
        graph.set_edge_value($V(t, d_1, v_1)$, $V(t+1, d_2, v_2)$, Fuel($v_1, v_2 - v_1, \theta_1$));
      end
    end
  end
end
Return Dijkstra(graph, $V(t_o, d_o, v_o)$, $V(t_d, d_d, v_d)$);

FIGURE 6 The three-intersection (red lines in the Google Map) corridor with detailed parameters (including spacing and signal timing plans). T_{s1} = 20 s (when the phase is red at Maybell Ave.) and T_{s2} = 70 s (when the phase is green at Maybell Ave.) represent the starting times of two testing scenarios.

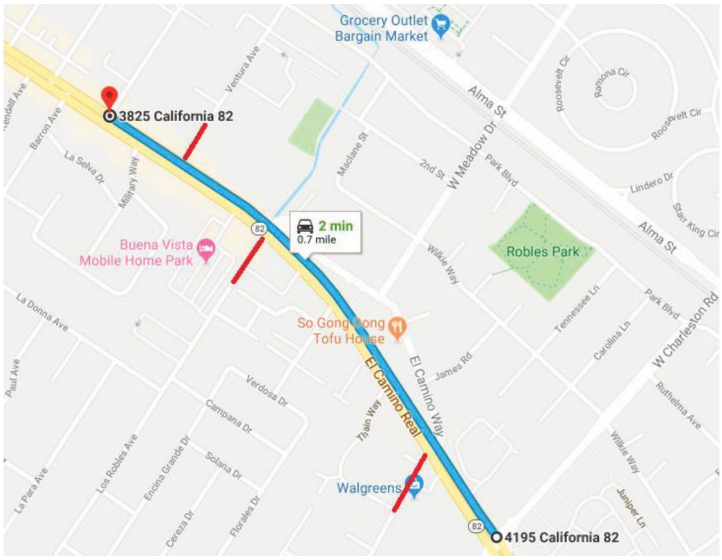

(a) Map of the numerical case study in Palo Alto, CA (Source: Google Map).

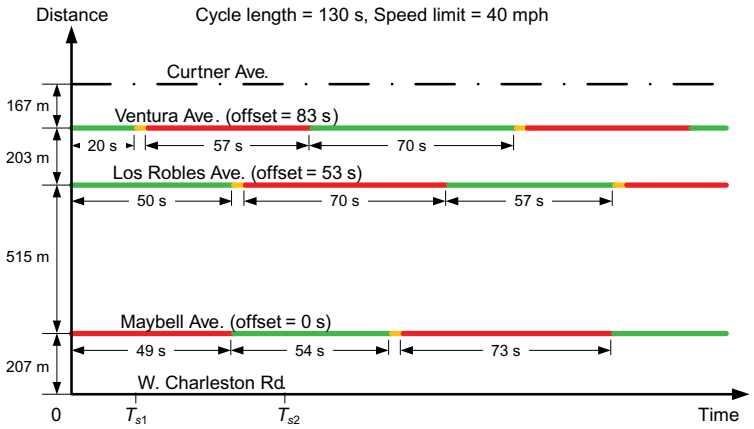

(b) SPaT of three intersections along El Camino Real in Palo Alto, CA.

we consider it as a flat segment. As shown in Figure 6(a), the intersection spacing within this stretch varies from 200 m to 500 m and the speed limit is 40 mph. The background signal timing plans (130 s of cycle length) at these three intersections for the northbound direction are illustrated in Figure 6(b), which were obtained from archived document by the California Department of Transportation (Caltrans) D4 and implemented in the field in July 2005.

We evaluate the performance of the proposed EADSC system with two scenarios. In both scenarios, the host vehicle starts off (northbound) from the landmark 207 m upstream of Maybell Ave., that is, from W. Charleston Rd. at El Camino Real, and terminates the trip at the intersection of Ventura Ave. with target speed of 40 mph. The starting times are T_{s1} = 20 s and T_{s2} = 70 s for Scenario 1 and Scenario 2, respectively (see Figure 6). As to the SPaT at Maybell Ave., Scenario 1 represents a typical case approaching in red (remaining time is 29 s), while Scenario 2 denotes the case approaching in green (remaining time is 33 s).

For comparison, we totally test five driving strategies as described in the following (see Figure 7):

1. Baseline driving strategy without the SPaT information (as "*Baseline*" in Figure 7). With this strategy, the host vehicle attempts to cruise at or around the speed limit unless getting close to the signalized intersections during the red phase (slowing down and stop if necessary).
2. Piecewise linear trigonometric function like eco-driving strategy (as "*Trigonometric EAD*" in Figure 7). Please refer to [12, 27] for more technical details.

FIGURE 7 Distance-time diagrams of five driving strategies under two scenarios in numerical simulation.

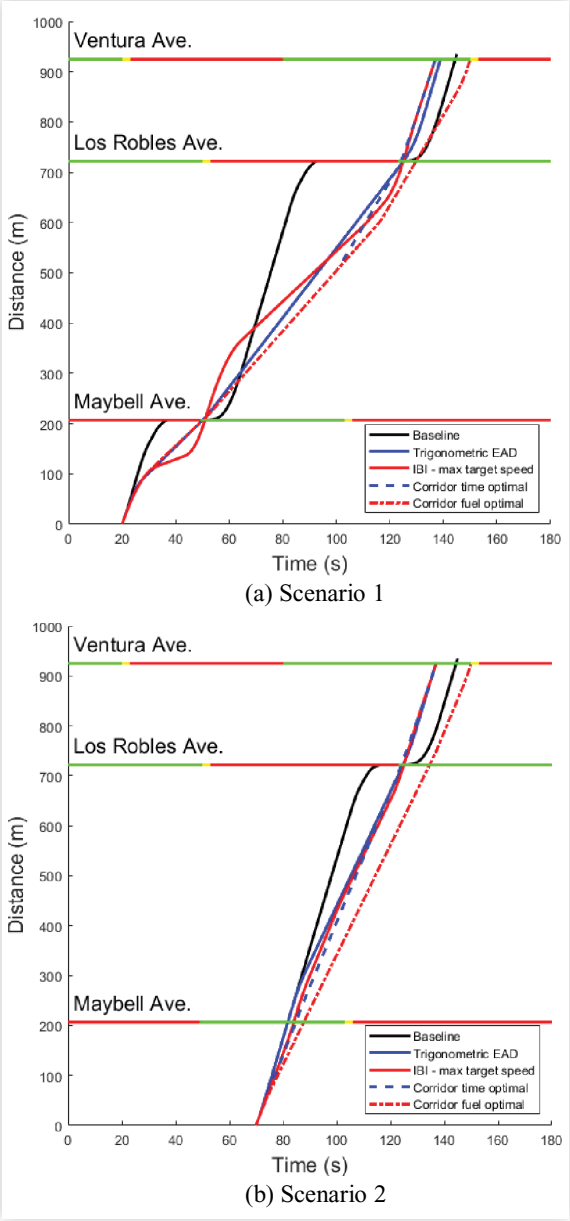

3. Intersection-by-intersection shortest-path-based eco-driving strategy with priority in travel time (as "IBI-*max target speed*" in Figure 7). This strategy is based on what we presented in the *vehicle trajectory planning* step (in Section 3.3). We define the target state at each intersection and consider the consistency between the end state of an upstream section and the initial state of the respective downstream section.
4. Corridor-wise shortest-path-based eco-driving strategy with priority in travel time (as "*Corridor time optimal*" in Figure 7). Based on the proposed EADSC algorithm, an optimal (in terms of minimizing the trip time) corridor-wise speed profile can be calculated with the specified target state at the end of the corridor.
5. Corridor-wise shortest-path-based eco-driving strategy with priority in fuel consumption (as "*Corridor fuel optimal*" in Figure 7). This strategy is also based on the proposed EADSC algorithm in this article. Rather than prioritizing the mobility performance, this strategy provides the corridor-wise optimal vehicle trajectory in terms of minimizing the fuel consumption, where target passage cycles are determined using the algorithm presented in Section 3.2.

It is noted that for both "*Baseline*" and "*Trigonometric EAD*" strategies, the jerk constraint suggested by [47] has been applied to guarantee the driving comfort. For the other three shortest path-based strategies, that is, "IBI-max target speed," "corridor time optimal," and "corridor fuel optimal," switching between drastic acceleration and deceleration is discouraged by the proposed model. Therefore, the jerk would be limited by the acceleration range as aforementioned (i.e., $-2\ \text{m/s}^2 \leq \text{accel} \leq 2\ \text{m/s}^2$).

We estimate the trip-level fuel consumption for all the strategies and the results are summarized in Table 1. As can be observed in the table, all eco-driving strategies can significantly reduce fuel consumption, compared to the baseline driving strategy. The improvement may range from 12% to 28%, depending on the scenario. Most of the eco-driving strategies (except for the corridor-wise fuel optimal eco-driving strategy, i.e., "Cor. Fuel") also outperform the baseline driving strategy in mobility performance. For the corridor-wise fuel-oriented eco-driving strategy, the host vehicle chooses the end of green window (at the intersection of Ventura Ave.) to achieve the fuel savings to the maximum extent in both scenarios.

Further comparison results reveal that: (a) Compared to "Trigonometric EAD" strategy, "*IBI-max target speed*" strategy performs better or at least the same in terms of mobility while the energy benefits or dis-benefits may vary with scenarios; (b) "*Corridor time optimal*" strategy can save up to 4.3% more fuels than "Trigonometric EAD" strategy in both scenarios, without compromising in trip time; (c) The corridor-wise eco-driving strategies always outperform the intersection-by-intersection strategy in terms of fuel savings (in the range of 4-9%), and "*corridor time optimal*" strategy can guarantee no penalty in mobility performance; (d) For different versions of corridor-wise eco-driving strategies (i.e., time-saving vs. fuel savings), fuel savings may be further squeezed out by 2-3% (around 0.01 liter in this study) but at the cost of travel time increase by up to 20% (about 13 s for both scenarios). This may shed some light upon the trade-offs between mobility and fuel/energy benefits regarding the proposed EADSC system.

5. Field Implementation

A field implementation with a real passenger vehicle is also conducted to validate the effectiveness of the proposed EADSC system. The testbed is located at the Federal Highway

TABLE 1 Comparison in performance measures for different driving strategies under two scenarios

		Fuel (liter)		Trip time (s)	
Scenario	**Strategy**	**Absolute**	**Change (%)**	**Absolute**	**Change (%)**
Scenario 1	Baseline	0.4641	—	124	—
	Trigonometry	0.3565	–23.2	119	–4.0
	Int-By-Int	0.3678	–20.8	117	–5.7
	Cor. Time	0.3428	–26.1	117	–5.7
	Cor. Fuel	0.3359	–27.6	130	4.8
Scenario 2	Baseline	0.4209	—	75	—
	Trigonometry	0.3706	–12.0	67	–10.7
	Int-By-Int	0.3595	–14.6	67	–10.7
	Cor. Time	0.3545	–15.8	67	–10.7
	Cor. Fuel	0.3439	–18.3	80	6.7

Administration's (FHWA) Turner-Fairbank Highway Research Center (TFHRC) in McLean, Virginia, using the Saxton Transportation Operations Laboratory (STOL) Intelligent Intersections. This testbed offers a sheltered traffic environment where the field test can be conducted with minimal safety risk and without disrupting live traffic operations.

Figure 8 provides an overview of this testbed, specifying the starting point (green pin) where the test vehicle can begin test runs from a stop and travel through two consecutive intersections (blue pins). The test corridor covers a range of approximately 320 m. The maximum allowable travel speed is 30 mph (13.41 m/s). Each of the two intersections is equipped with a McCain ATC2 traffic controller, which sends out SPaT objects in the NTCIP 1202 standard. To allow the test vehicle to receive this information, the DSRC J2735 Map and SPaT messages are broadcasted from a Cohda MK5 RSUs mounted at each intersection. The forwarding of the Map and SPaT messages to the RSU is handled using the open source software V2XHub [48]. Both traffic signal controllers are set up for fixed-time signal plans (i.e., green for 27 s, yellow for 3 s, and red for 30 s in each cycle along the travel direction), which removes excess all-red clearance timings and loop detector triggers from actuating the signal.

The test vehicle is a production Cadillac SRX 2013 (shown in Figure 9), which is outfitted for automated throttle and brake control using hardware developed by STOL and TORC Robotics. It is additionally equipped with a TORC PinPoint GPS unit, which integrates IMU and Dual Phase GPS solution for accurate localization.

The algorithm implementation is built as a plugin for the CARMA Platform (Ver. 2.8.1) software package [49]. The CARMA Platform is an Open Source Software platform developed at STOL, and is designed to support research in Cooperative Automation. The platform is built on top of the Robot Operating System (ROS) supporting level 1 speed control [50]. Different cooperative algorithms are implemented as Java plugins, which provide speed commands to

FIGURE 8 Field implementation testbed at the FHWA Turner-Fairbank Highway Research Center in McLean, VA. Start and end points are shown as green and red pins, respectively. Two intersection center points are shown as blue pins (Source: Google Map).

Map Data: © 2020 Google. Imagery: © 2020 CNES/Airbus Commonwealth of Virginia, Maxar Technologies, Sanborn, U.S Geological Survey

FIGURE 9 The test vehicle running the algorithm using the CARMA Platform (Source: FHWA).

Reprinted from Federal Highway Administration

the vehicle through the CARMA Platform APIs. A diagram of the CARMA Platform system architecture showing where the plugins fit is shown in Figure 10.

Two representative runs from different directions (i.e., eastbound and westbound) in the field implementation are illustrated in Figures 11 and 12, respectively, where the D-T plots and speed trajectories are presented. In Run 1, the D-T plot (see Figure 11(a)) shows the test vehicle first accelerates to catch up with the end of green phase (with some safety buffer time) at the first traffic signal, thus no full stop is needed and the fuel consumption can be saved.

For the second traffic signal, the vehicle cruises through the intersection during the green phase without any speed changes. Figure 11(b) illustrates the speed trajectories of this scenario, where both the "commanded speed" profile and "vehicle speed" profile are shown. The "commanded speed" profile is calculated by the proposed algorithm with real-time feedback update (e.g., considering cumulative errors in the speed tracking), while the "vehicle speed" profile is the output from the actuator.

In Run 2 as shown in Figure 12, when approaching both traffic signals, the test vehicle slightly decelerates during the red phase, and passes both intersections at the beginning of the green phases (with some safety buffer time). In this manner, the test vehicle may avoid full stops and unnecessary idling at the intersections, and arrives just in time when the signal turns from red to green.

6. Discussion

In this section, we will further discuss some practical issues related to the real-world deployment of the proposed corridor-wise EAD application.

6.1. Availability of Signal Timing Plan

Most of the existing studies on EAD have assumed that the equipped vehicle has the knowledge about the signal timing plan at the intersection, including cycle length, phase duration, and sequence, which is not readily available in the SPaT message. This would give rise to additional challenges for the implementation of EAD application.

FIGURE 10 High-level CARMA Platform v2.8.1 architecture (Source: FHWA).

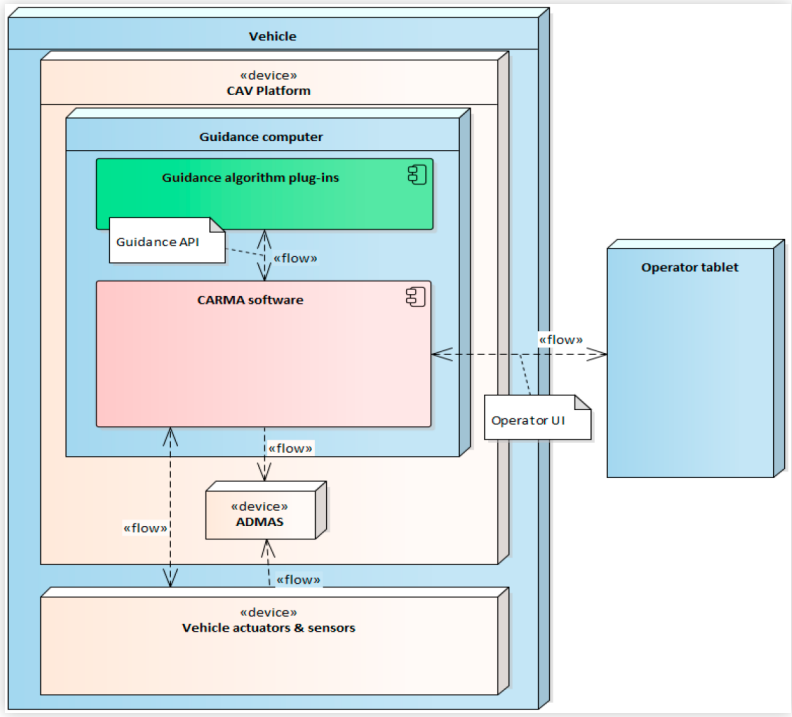

Reprinted from Ref. [x]

FIGURE 11 Distance-time plot and speed trajectory of Run 1.

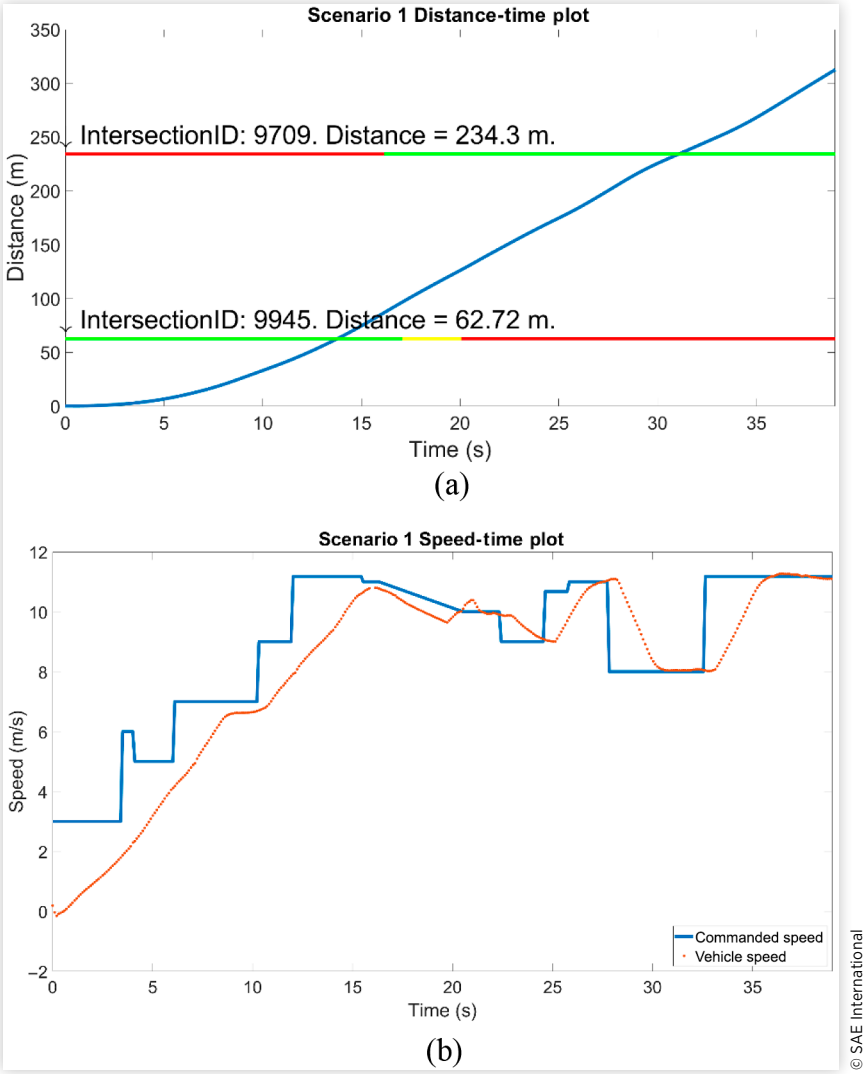

In the United States, the art-of-the-practice traffic signal control organizes phases by grouping them into rings and separating the conflicting traffic streams either by making the movements sequential or adding barriers in between [51]. Figure 13 presents an example of the ring-and-barrier diagram to illustrate the time sequence of phases. At each time step, the available information from SPaT messages includes the current phase (i.e., green, yellow, red, or maybe all-red clearance) and minimum/maximum time of change to the next phase [43]. For example (see Figure 13), assuming that the host vehicle is approaching the intersection along the through lane (i.e., Movement #2) at time t_0, it knows the current phase through movement being green, and can obtain the time instances of all movements when the associated next phases start or $T2N_i$'s (where i represents the movement index). With this limited information, the host vehicle is able to know the (exact) end time of current green and a lower bound of time-to-next-green (i.e., $T2NG_2$). Unless it keeps tracking the SPaT for a certain period, the host vehicle would not have a complete knowledge of all the downstream signal timings to plan well its trajectory even under fixed-time signal control. To mitigate this issue, the signal timing plan should be broadcast, or a separate on-board module needs to be developed to learn the background signal control parameters and predict the operation of signal controllers.

Toward this end, we may modify the way to construct the RR (in a conservative manner) for an isolated intersection based on the partial knowledge of signal plan. Here, we take an example where the host vehicle approaches the intersection in green (at time t_0). Based on the on-board radar detection (with the range R_r), we can construct the reliable RR (assuming no cut-ins by other vehicles). In addition, a predicted RR can be constructed based on the information available (if any) from the V2I communication range R_c (assuming a limited

FIGURE 12 Distance-time plot and speed trajectory of Run 2.

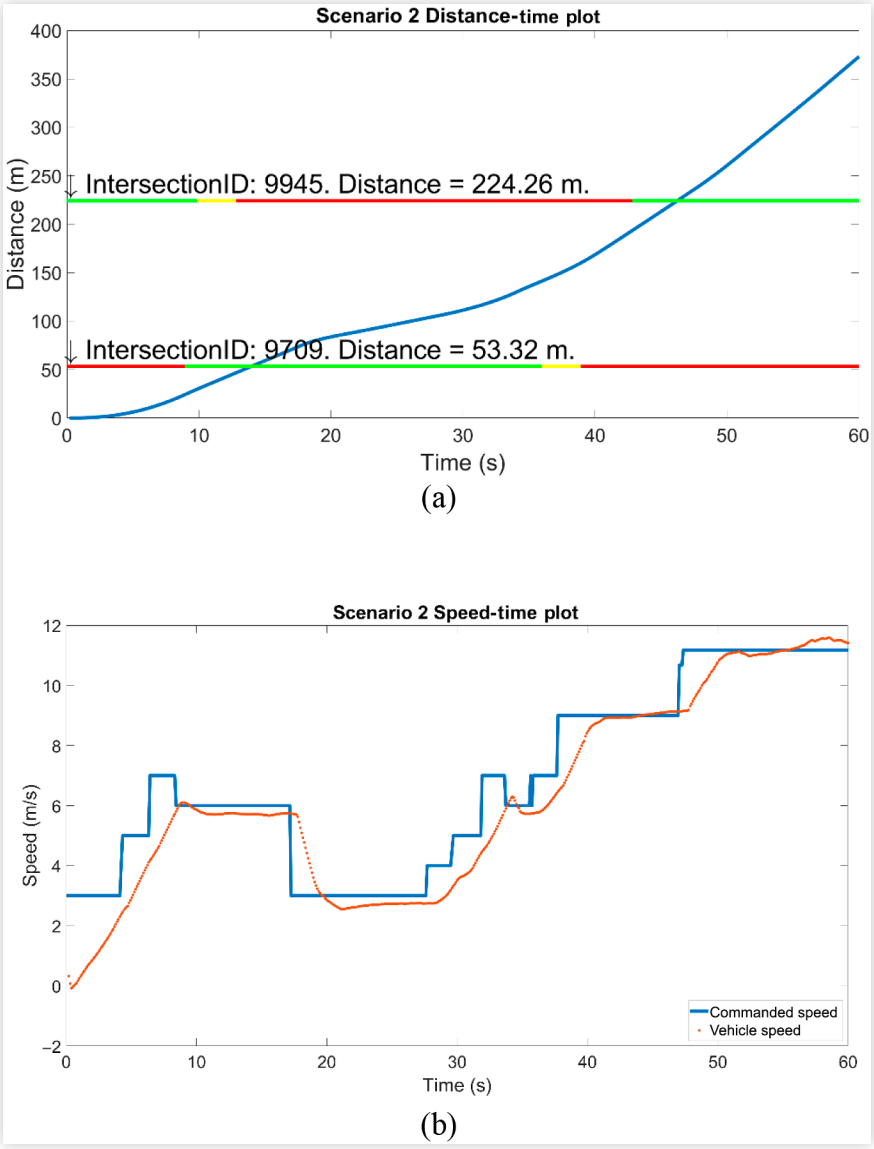

communication range). If the vehicle is predicted to be able to pass through the intersection in current green (constrained by the host vehicle's maximum power/acceleration and predicted trajectories of other vehicles), then the predicted RR will include area in the downstream of the intersection. Otherwise, the predicted RR will be restricted to the upstream of the intersection as shown in Figure 14, where the length of red phase is unknown and is assumed to be long (or at least longer than *T2N4* in Figure 13). The detected preceding (nonconnected) vehicles are predicted to be stopped in the queue or at the stop line.

6.2. Other Traffic Interaction

In this article, we mainly focus on the description of the EADSC, comparative results with other algorithms and prototyping efforts in idealized scenarios. Although the *RR construction* module may cover some practical issues (e.g., with downstream traffic detection and prediction), more delicate interaction with other traffic such as cut-ins and wrecks would further complicate the proposed system. In these unexpected situations, the ego-vehicle may need to apply emergency stops or make lane changes to avoid any safety risks or getting stuck behind a queue, and re-optimize its speed trajectories based on the updated information. As mentioned in Section 3.1, the lane-level *RR construction* module developed in this study can also accommodate some realistic traffic interaction and can further integrate with lateral control/maneuvers to enable more advanced eco-driving strategies (e.g., queue balancing or overtaking) along the signalized corridor.

FIGURE 13 An example of the ring-and-barrier diagram.

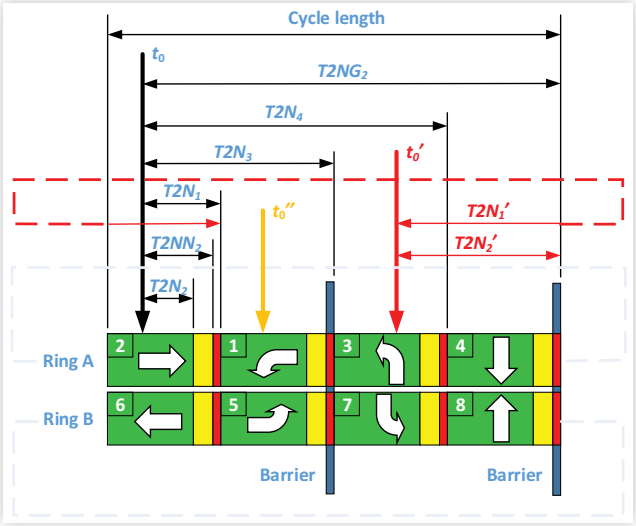

7. Conclusions and Future Work

In this study, we proposed an innovative algorithm for EADSC, featured with three major steps, that is, *RR construction*, *target cycle determination*, and *vehicle trajectory planning*. Results from the numerical simulation on a real-world three-intersection corridor showed great potential of the proposed EADSC in terms of fuel savings without compromising the mobility benefits, compared to the baseline driving strategy without knowing the SPaT information (by up to 28%) as well as the trigonometric function like EAD strategy (by around 4.3%) that was previously developed by the authors. Using the same vehicle trajectory planning algorithm, further energy benefits (ranging from 4% to 9%) could be squeezed out based on the knowledge of corridor-wise signal timing plans rather than using the SPaT information on an intersection basis. A field implementation with real passenger vehicle also validates the effectiveness of the proposed EADSC system. In addition, we discuss some issues for real-world implementation of the system, including the availability of only partial knowledge about downstream signal information from current SPaT messages, and the presence of more realistic traffic interaction.

Potential work on the proposed EADSC system would be focused on the validation in more complex environments. These may include handling intersections with actuated and adaptive signals, as well as combination with platooning operations. Other opportunities for additional research include (a) the application of this algorithm in mixed traffic scenarios (i.e., with other legacy vehicles or connected but manually driven vehicles); (b) the integration with queue prediction technique and lateral control; (c) the consideration of imperfect positional accuracy (e.g., under "urban canyon" situations); and (d) the modifications for case(s) of right-turn on red (RTOR) or permissive left-turn. Testing and validation of the proposed EADSC system in a microscopic traffic environment such as SUMO or Vissim would, to certain degree, help better understand the aforementioned issues and prepare for more sophisticated field deployment.

FIGURE 14 An example of modified reachable region in D-T diagram when the host vehicle is approaching the intersection in green.

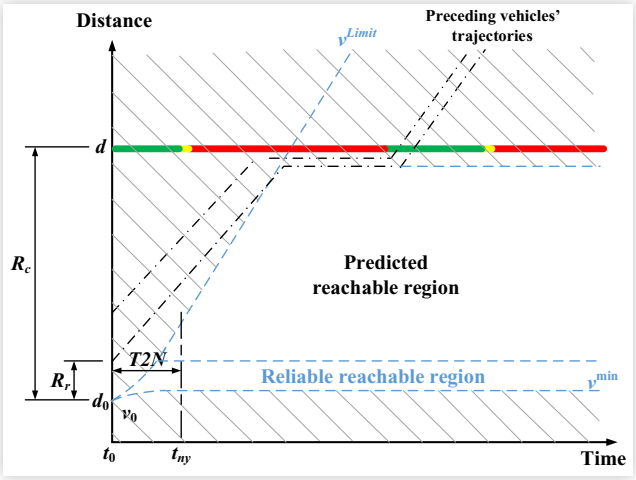

Contact Information

Guoyuan Wu, PhD
Center for Environmental Research & Technology,
University of California at Riverside
gywu@cert.ucr.edu

Acknowledgments

This research is supported by the Federal Highway Administration (FHWA). The contents of this article reflect the viewpoints of the authors, who are responsible for the facts and the accuracy of the data presented, and do not necessarily reflect the viewpoints of the FHWA or the U.S. Department of Transportation.

References

1. U.S. Energy Information Administration, "Use of Energy Explained," https://www.eia.gov/energyexplained/use-of-energy/transportation.php, accessed 15 Sep. 2020.
2. U.S. Environmental Protection Agency (USEPA), "Inventory of U.S. Greenhouse Gas Emissions and Sinks 1990-2018," Apr. 2020, https://www.epa.gov/sites/production/files/2020-04/documents/us-ghg-inventory-2020-main-text.pdf, accessed 15 Sep. 2020.
3. U.S. Department of Transportation (USDOT), "Applications for the Environment: Real-Time Information Synthesis,"

https://www.its.dot.gov/research_archives/aeris/index.htm, accessed July 15, 2019.

4. European Commission (EC), "eCoMove—Cooperative Mobility Systems and Services for Energy Efficiency," http://www.ecomove-project.eu/, accessed July 15, 2019.
5. European Commission (EC), "Horizon 2020," ec.europa.eu/programmes/horizon2020/en/h2020-section/smart-green-and-integrated-transport, accessed July 15, 2019.
6. USDOT, "Connected Vehicle Reference Implementation Architecture (CVRIA) Version 2," https://www.its.dot.gov/research_archives/arch/cvria2.htm, accessed July 15, 2019.
7. USDOT, "Environment—Eco Approach and Departure at Signalized Intersections," https://www.its.dot.gov/infographs/Eco_approach_departure.htm, accessed July 15, 2019.
8. Li, M., Boriboonsomsin, K., Wu, G., Zhang, W. et al., "Traffic Energy and Emission Reductions at Signalized Intersections: A Study of the Benefits of Advanced Driver Information," *International Journal of ITS Research* 7(1):49-58, 2009.
9. Wu, G., Boriboonsomsin, K., Zhang, W.-B., Li, M. et al., "Energy and Emission Benefit Comparison between Stationary and In-Vehicle Advanced Driving Alert Systems," *Transportation Research Record: Journal of the Transportation Research Board* 2189:98-106, 2010.
10. Katsaros, K., Kernchen, R., Dianati, M., and Rieck, D., "Performance Study of a Green Light Optimized Speed Advisory (GLOSA) Application Using an Integrated Cooperative ITS Simulation Platform," in *The 7th International Wireless Communications and Mobile Computing Conference*, Istanbul, Turkey, July 2011.
11. Garcia-Castro, A., Monzon, A., Valdes, C., and Romana, M., "Modeling Different Penetration Rates of Eco-Driving in Urban Areas: Impacts on Traffic Flow and Emissions," *International Journal of Sustainable Transportation* 11(4):282-294, 2017.
12. Mandava, S., Boriboonsomsin, K., and Barth, M., "Arterial Velocity Planning Based on Traffic Signal Information under Light Traffic Conditions," in *The 12th International IEEE Conference on Intelligent Transportation Systems*, St. Louis, MO, Oct. 2009.
13. Kamal, M.A.S., Mukai, M., Murata, J., and Kawabe, T., "Ecological Driver Assistance System Using Model Based Anticipation of Vehicle-Road-Traffic Information," *IET Journal of Intelligent Transportation Systems* 4(4):244-251, 2010.
14. Rakha, H. and Kamalanathsharma, R., "Eco-Driving at Signalized Intersections Using V2I Communication," in *The 14th IEEE Conference on Intelligent Transportation Systems (ITSC)*, Washington, DC, Oct. 2011.
15. Asadi, B. and Vahidi, A., "Predictive Cruise Control: Utilizing Upcoming Traffic Signal Information for Improving Fuel Economy and Reducing Trip Time," *IEEE Transactions on Control Systems Technology* 19(3):707-714, 2011.
16. Katsaros, K., Kernchen, R., Dianati, M., Rieck, D. et al., "Application of Vehicular Communications for Improving the Efficiency of Traffic in Urban Areas," *Wireless Communications and Mobile Computing* 11:1657-1667, 2011.
17. Chen, Z., Zhang, Y., Lv, J., and Zou, Y., "Model for Optimization of Eco-Driving at Signalized Intersections," *Transportation Research Record* 2427:54-62, 2014.
18. Jin, Q., Wu, G., Boriboonsomsin, K., and Barth, M., "Power-Based Optimal Longitudinal Control for a Connected Eco-Driving System," *IEEE Transactions on Intelligent Transportation Systems* 17(10):2900-2910, 2016.
19. Li, S., Xu, S., Huang, X., Cheng, B. et al., "Eco-Departure of Connected Vehicles with V2X Communication at Signalized Intersections," *IEEE Transactions on Vehicular Technology* 64(12):5439-5449, 2015.
20. Huang, X. and Peng, H., "Speed Trajectory Planning at Signalized Intersections with Sequential Convex Optimization," in *Proceedings of the 2017 American Control Conference*, Seattle, WA, 2017.
21. Huang, K., Yang, X., Lu, Y., Mi, C. et al., "Ecological Driving System for Connected/Automated Vehicles Using a Two-Stage Control Hierarchy," *IEEE Transactions on Intelligent Transportation Systems* 19(7):2373-2384, 2018.
22. Yang, H., Almutairi, F., and Rakha, H., "Eco-Driving at Signalized Intersections: A Multiple Signal Optimization Approach," *IEEE Transactions on Intelligent Transportation Systems*, 2020, https://doi.org/10.1109/TITS.2020.2978184 (Early Access).
23. Xia, H., "K. Boriboonsomsin, and M. Barth, Dynamic Eco-Driving for Signalized Arterial Corridors and Its Indirect Network-Wide Energy/Emissions Benefits," *Journal of Intelligent Transportation Systems* 17:31-41, 2013.
24. Xia, H., Boriboonsomsin, K., Schweizer, F., Winckler, A. et al., "Field Operational Testing of ECO-Approach Technology at a Fixed-Time Signalized Intersection," in *The 15th IEEE Intelligent Transportation Systems Conference*, Anchorage, AK, Sept. 2012.
25. Wang, Z., Hsu, Y.-P., Vu, A., Caballero, F. et al., "Early Findings from Field Trials of Heavy-Duty Truck Connected Eco-Driving System," in *2019 22th International IEEE Conference on Intelligent Transportation Systems (ITSC)*, Auckland, New Zealand, Oct. 2019, 3037-3042.
26. Wu, G., Boriboonsomsin, K., Xia, H., and Barth, M., "Supplementary Benefits from Partial Vehicle Automation in an Eco-Approach and Departure Application at Signalized Intersections," *Transportation Research Record: Journal of the Transportation Research Board* 2424:66-75, 2014.
27. Altan, O., Wu, G., Barth, M., Boriboonsomsin, K. et al., "GlidePath: Eco-Friendly Automated Approach and Departure at Signalized Intersections," *IEEE Transactions on Intelligent Vehicles* 2(4):266-277, 2017.
28. Kamalanathsharma, R. and Rakha, H., "Multi-Stage Dynamic Programming Algorithm for Eco-speed Control at Traffic Signalized Intersections," in *The 16th International IEEE Conference on Intelligent Transportation Systems*, the Hague, Netherlands, Oct. 2013.
29. Wan, N., Vahidi, A., and Luckow, A., "Optimal Speed Advisory for Connected Vehicles in Arterial Roads and the

Impact on Mixed Traffic," *Transportation Research Part C* 69:548-563, 2016.

30. Jiang, H., Hu, J., An, S., Wang, M. et al., "Eco Approaching at an Isolated Signalized Intersection under Partially Connected and Automated Vehicles Environment," *Transportation Research Part C* 79:290-307, 2017.
31. He, X., Liu, H., and Liu, X., "Optimal Vehicle Speed Trajectory on a Signalized Arterial with Consideration of Queue," *Transportation Research Part C: Emerging Technology* 61:106-120, 2015.
32. Ye, F., Hao, P., Qi, X., Wu, G. et al., "Prediction-Based Eco-Approach and Departure at Signalized Intersections with Speed Forecasting on Preceding Vehicles," *IEEE Transactions on Intelligent Transportation Systems* 20(4):1378-1389, 2019.
33. Mahler, G. and Vahidi, A., "An Optimal Velocity-Planning Scheme for Vehicle Energy Efficiency through Probabilistic Prediction of Traffic-Signal Timing," *IEEE Transactions on Intelligent Transportation Systems* 15:2516-2523, 2014.
34. Hao, P., Wu, G., Boriboonsomsin, K., and Barth, M., "Eco-Approach and Departure (EAD) Application for Actuated Signals in Real-World Traffic," *IEEE Transactions on Intelligent Transportation Systems* 20(1):30-40, 2019.
35. Sun, C., Shen, X., and Moura, S., "Robust Optimal Eco-driving Control with Uncertain Traffic Signal Timing," in *2018 Annual American Control Conference (ACC)*, Milwaukee, WI, 2018.
36. Hao, P., Wei, Z., Bai, Z., and Barth, M., "Developing an Adaptive Strategy for Connected Eco-Driving Under Uncertain Traffic and Signal Conditions," NCST Research Report, 2020, https://doi.org/10.7922/G2F18WZ1.
37. Ozatay, E., Ozguner, U., Filev, D. and Michelini, J., "Analytical and Numerical Solutions for Energy Minimization of Road Vehicles with the Existence of Multiple Traffic Lights," in *The 52nd IEEE Conference on Decision and Control*, Firenze, Italy, 2013, IEEE.
38. Lin, Q., Du, X., Li, S., and Ye, Z., "Vehicle-to-Infrastructure Communication Based Eco-Driving Operation at Multiple Signalized Intersections," in *2016 IEEE Vehicle Power and Propulsion Conference*, Hangzhou, China, Dec. 2016, https://doi.org/10.1109/VPPC.2016.7791809.
39. De Nunzio, G., Canudas De Wit, C., Moulin, P., and Di Domenico, D., "Eco-Driving in Urban Traffic Networks Using Traffic Signals Information," *International Journal of Robust and Nonlinear Control* 26:1307-1324, 2016.
40. Zhao, X., Wu, X., Xin, Q., Sun, K. et al., "Dynamic Eco-Driving on Signalized Arterial Corridors during the Green Phase for the Connected Vehicles," *Journal of Advanced Transportation* 2020:Article ID 1609834, 2020, https://doi.org/10.1155/2020/1609834.
41. Ross, M., "Fuel Efficiency and the Physics of Automobiles," *Contemporary Physics* 38(6):381-394, 1997.
42. Hao, P., Boriboonsomsin, K., Wang, C., Wu, G. et al., "Connected Eco-Approach and Departure (EAD) System for Diesel Trucks," *SAE International Journal of Commercial Vehicles* (in press).
43. SAE International, "J2735—Dedicated Short Range Communications (DSRC) Message Set Dictionary," Mar. 2016.
44. Wu, G., Hao, P., Wang, Z., Boriboonsomsin, K. et al., "Eco-Approach and Departure along Signalized Corridors," Presentation at in *the 98th Annual Meeting of Transportation Research Board*, Washington, DC, Jan. 2019.
45. Dijkstra, E.W., "A Note on Two Problems in Connexion with Graphs," *Numerische Mathematik* 1:269-271, 1959.
46. Hart, P.E., Nilsson, N.J., and Raphael, B.A., "Formal Basis for the Heuristic Determination of Minimum Cost Paths," *IEEE Transactions on Systems Science and Cybernetics* 4(2):100-107, 1968.
47. Yi, K. and Chung, J., "Nonlinear Brake Control for Vehicle CW/CA Systems," *IEEE/ASME Transactions on Mechatronics* 6(1):17-25, 2001.
48. FHWA, "V2X Hub," https://github.com/usdot-fhwa-OPS/V2X-Hub.
49. FHWA, "CARMA," https://github.com/usdot-fhwa-stol/CARMAPlatform (Version_2.8.1).
50. Quigley, M., Conley, K., Gerkey, B. et al., "ROS: An Open-Source Robot Operating System," in *ICRA Workshop on Open Source Software*, Kobe, Japan, May 12-17, 2009.
51. Gordon, R., "Traffic Signal Retiming Practices in the United States," NCHRP Synthesis 409, Published by Transportation Research Board, Washington, DC, 2010.